Molecular Imaging
Volume 16: 1-10

DOI: 10.1177/1536012117737399
journals.sagepub.com/home/mix
SAGE

Radiolabeled Anti-Adenosine Triphosphate Synthase Monoclonal Antibody as a Theragnostic Agent Targeting Angiogenesis

Bok-Nam Park, PhD[1], Su Jin Lee, MD, PhD[1], Jung Hyun Roh, MS[1], Kyung-Han Lee, MD, PhD[2], Young-Sil An, MD, PhD[1], and Joon-Kee Yoon, MD, PhD[1]

Abstract

Introduction: The potential of a radioiodine-labeled, anti-adenosine triphosphate synthase monoclonal antibody (ATPS mAb) as a theragnostic agent for simultaneous cancer imaging and treatment was evaluated.

Methods: Adenosine triphosphate synthase monoclonal antibody was labeled with radioiodine, then radiotracer uptake was measured in 6 different cancer cell lines. In vivo biodistribution was evaluated 24 and 48 hours after intravenous injection of ^{125}I-ATPS mAb into MKN-45 tumor-bearing mice (n = 3). For radioimmunotherapy, 18.5 MBq ^{131}I-ATPS mAb (n = 7), isotype immunoglobulin G (IgG) (n = 6), and vehicle (n = 6) were injected into MKN-45 tumor-bearing mice for 4 weeks, and tumor volume and percentage of tumor growth inhibition (TGI) were compared each week.

Results: MKN-45 cells showed the highest in vitro cellular binding after 4 hours (0.00324 ± 0.00013%/μg), which was significantly inhibited by unlabeled ATPS mAb at concentrations of greater than 0.4 μM. The in vitro retention rate of ^{125}I-ATPS mAb in MKN-45 cells was 64.1% ± 1.0% at 60 minutes. The highest tumor uptake of ^{125}I-ATPS mAb in MKN-45 tumor-bearing mice was achieved 24 hours after injection (6.26% ± 0.47% injected dose [ID]/g), whereas tumor to muscle and tumor to blood ratios peaked at 48 hours. The 24-hour tumor uptake decreased to 3.43% ± 0.85% ID/g by blocking with unlabeled ATPS mAb. After 4 weeks of treatment, mice receiving ^{131}I-ATPS mAb had significantly smaller tumors (679.4 ± 232.3 mm^3) compared with control (1687.6 ± 420.4 mm^3, $P = .0431$) and IgG-treated mice (2870.2 ± 484.1 mm^3, $P = .0010$). The percentage of TGI of ^{131}I-ATPS mAb was greater than 50% during the entire study period (range: 53.7%-75.9%).

Conclusion: The specific binding and antitumor effects of radioiodinated ATPS mAb were confirmed in in vitro and in vivo models of stomach cancer.

Keywords

adenosine triphosphate synthase, angiogenesis, radioimmunotherapy, monoclonal antibody, iodine radioisotopes

Introduction

Solid tumors require new vessel formation, a process called angiogenesis, to grow and metastasize.[1] Whether tumor growth is aggravated or inhibited is dependent on the balance between proangiogenic and antiangiogenic factors. Angiostatin is a potent, intrinsic antiangiogenic factor that can reverse the "angiogenic switch."[2]

Researchers have found that adenosine triphosphate (ATP) synthase is not only located in the mitochondrial inner membrane but also on the surface membrane of endothelial and tumor cells.[3,4] Ectopic ATP synthase α/β subunits have been

[1] Department of Nuclear Medicine and Molecular Imaging, Ajou University School of Medicine, Suwon, South Korea
[2] Department of Nuclear Medicine and Molecular Imaging, Samsung Medical Center, Sungkyunkwan University School of Medicine, Seoul, South Korea

Submitted: 08/12/2016. Revised: 17/04/2017. Accepted: 29/04/2017.

Corresponding Author:
Joon-Kee Yoon, Department of Nuclear Medicine and Molecular Imaging, Ajou University School of Medicine, 164 Worldcup-ro, Yeongtong-gu, Suwon 16499, South Korea.
Email: jkyoon3@ajou.ac.kr

confirmed experimentally as a binding site for angiostatin; therefore, ectopic ATP synthase is a potential target of antiangiogenic therapy.[5] Angiostatin itself inhibits the ATP hydrolytic activity of F_1 ATP synthase (extramembranous component); in addition, a polyclonal antibody against the α-subunit of ATP synthase blocked the binding of angiostatin and abrogated its inhibitory effect on endothelial proliferation.[3,6] A monoclonal antibody to the β catalytic subunit of ATP synthase inhibited the hydrolytic activity and ATP generation by ATP synthase on the surface of endothelial cells, consequently disrupting endothelial cell tube formation and neovascularization.[7] Moreover, preventing ATP synthase activity can prevent the proliferation and migration of breast cancer cells and enhance the cytotoxic effects of doxorubicin.[8] Thus, monoclonal antibodies against ATP synthase are good candidates for antiangiogenic treatment.

Radioimmunotherapy has become a promising anticancer strategy ever since the therapeutic efficacy of a specific carcinoembryonic antigen-radiolabeled antibody was reported in 1981.[9] Among the various radioisotopes, radioiodine was the first to be used as an antibody-linked label for imaging and therapeutic purposes.[10,11] The 4 different iodine radioisotopes have distinguishing physical characteristics that are useful for in vitro analyses (^{125}I), ex vivo biodistribution (^{125}I), in vivo imaging (^{123}I, ^{124}I, and ^{131}I), and therapy (^{131}I). Therefore, radioiodine-labeled antibodies are a prime example of a theragnostic radiopharmaceutical.

With regard to the imaging of F_1F_O ATP synthase using radioisotopes, researchers have already demonstrated that radioiodine-labeled angiostatin can be used for this purpose.[12-14] However, a direct labeling method showed limited in vivo stability, and a modified labeling method using a Bolton-Hunter reagent exhibited insufficient labeling efficiency; thus, the method still needs some improvement.[12,13]

Therefore, in the present study, an anti-ATP synthase monoclonal antibody (ATPS mAb) was labeled,[8] and its potential as an angiogenesis-targeting theragnostic agent was evaluated through in vitro and in vivo analyses.

Materials and Methods

Radioiodination of ATPS mAb

Adenosine triphosphate synthase monoclonal antibody was purchased from Abcam (MW 52 kDa, Cambridge, Massachusetts) and stored as aliquots at −78°C. Na^{125}I and Na^{131}I were obtained from PerkinElmer (Waltham, Massachusetts) and the Korea Atomic Energy Research Institute (Daejeon, Korea), respectively. For radioiodination, the Iodogen tube (Pierce Biotechnology, Rockford, Illinois) method was applied as described previously.[15] Briefly, 40 μg (5-80 μg) ATPS mAb was incubated with 185 MBq ^{125}I or ^{131}I (in phosphate-buffered saline [PBS], pH 7.4) in an Iodogen precoated tube (50 μg) for 25 minutes at room temperature. The radiolabeled antibody was purified by gel filtration on a PD-10 column (GE Healthcare Bio-Sciences AB, Uppsala, Sweden) and eluted with PBS. Two or 3 tubes with the highest radioactivity were combined for further experiments and labeling efficiency calculation.

Cell Lines and Xenograft Tumor Model

All cancer cell lines were obtained from the Korean Cell Line Bank (Seoul, Korea). All cells were grown in Dulbecco's modified Eagle's medium (high glucose; WelGENE Inc, Daegu, Korea) or RPMI-1640 medium (WelGENE Inc) supplemented with 10% fetal bovine serum (WelGENE Inc) and 1% penicillin/streptomycin at 37°C and 5% fully humidified CO_2. Animal experiments were performed according to protocols approved by the Care of Experimental Animals Committee (IACUC No. 2014-0040).[16,17] Six-week-old female Balb/c nude mice (Orient, Seongnam, Korea) were maintained under specific pathogen-free conditions. To induce xenografts, 1×10^6 tumor cells in phenol red-free Matrigel (BD Biosciences, Franklin Lakes, New Jersey) were injected subcutaneously into the dorsal region of the right thigh of each mouse. Experiments were performed ~10 to 14 days after injection, and the tumor size was 5 to 10 mm in diameter.

Cellular Uptake and Retention Rates of ^{125}I-ATPS mAb in MKN-45 Cells

Cellular uptake of ^{125}I-ATPS mAb was measured in the following 5 human cancer cell lines from different organs and 1 rat cancer cell line: MKN-45 (human gastric adenocarcinoma), HT-29 (human colorectal adenocarcinoma), PC-3 (human prostate adenocarcinoma), RR1022 (rat fibrosarcoma), SNU-449 (human hepatoma), and A549 cells (human lung adenocarcinoma). In total, 5×10^5 cells were seeded per well in 12-well plates and cultured overnight. Upon attachment, 18.5 kBq ^{125}I-ATPS mAb (5 ng/mL antibody) was added to freshly replaced culture media,[12,13] and cells were then incubated for 1, 2, or 4 hours at 37°C and 5% CO_2. After incubation, the cells were washed twice with cold PBS and harvested with 0.1 N NaOH. Radioactivity of the cells was counted using a Cobra II multichannel γ counter (PerkinElmer Inc) and normalized to cell protein content obtained using the Bradford method.[18]

For the measurement of retention rates, MKN-45 cells were cultured in 12-well plates and incubated with 18.5 kBq ^{125}I-ATPS mAb for 4 hours. After incubation, culture media were collected and changed after 0, 5, 10, 20, 30, and 60 minutes. The radioactivities of the supernatants from cells at each time point were measured using a γ counter. The retention rates of ^{125}I-ATPS mAb in MKN-45 cells were calculated and expressed as a relative percentage compared with cellular uptake at the 0 minute time point.

Specific Inhibition of ^{125}I-ATPS mAb by Unlabeled ATPS mAb in MKN-45 Cells

MKN-45 cells were cultured in 12-well plates and pretreated with 0 (untreated control), 0.1, 0.4, 1.6, or 6.4 μM unlabeled ATPS mAb for 1 hour; 18.5 kBq 125I-ATPS mAb was then

added to cells and incubated for 24 hours under the same conditions. After incubation, cellular uptake was calculated and expressed as a percentage relative to that of untreated control. Cellular uptake, retention, and inhibition experiments were performed in triplicate.

Western Blot Analysis for ATP Synthase in MKN-45 Cells

For Western blot analysis of anti-ATPS mAb, total membrane proteins and plasma membrane proteins were extracted using Minute plasma membrane protein isolation kit (Invent Biotechnologies, Inc, Plymouth, Minnesota) according to the manufacturer's instruction. The protein content was measured using a microplate reader and the Pierce-660 solution (Thermo Fisher Scientific, Waltham, Massachusetts). Samples (5 μg) were loaded on a 12% polyacrylamide gel and transferred to nitrocellulose membranes (Hybond ECL; Amersham Biosciences, Piscataway, New Jersey). The membranes were blocked with 5% skim milk and incubated overnight with anti-ATPS mAb at 4°C and then with an horseradish peroxide-linked secondary antibody (1:5000; Amersham Bioscience). The protein bands were finally visualized with enhanced chemiluminescence reagents (Amersham Bioscience) and exposure to an X-ray film (Agfa, Mortsel, Belgium). The intensity of bands was measured using ImageJ software (version 1.5).

In Vivo γ Camera Imaging, Biodistribution Study, and Blocking Study of ^{125}I-ATPS mAb in MKN-45 Tumor-Bearing Mice

For γ camera imaging, MKN-45 tumor-bearing mice (n = 5) were injected intravenously with 3.7 MBq ^{125}I-ATPS mAb (1 μg antibody). At 2, 24, and 48 hours after injection, static planar images were acquired using a γ camera (Orbiter; Siemens, Erlangen, Germany) fitted with a pinhole collimator (Siemens). Mice were scanned for 20 minutes in a prone position under inhalation anesthesia using isoflurane, and the matrix size was 256 × 256.

MKN-45 tumor-bearing mice (n = 3 for each time point) received an injection of 1.85 MBq ^{125}I-ATPS mAb through the tail vein and were killed for biodistribution at 24 and 48 hours after injection. Major organs as well as blood and tumors were dissected, weighed, and counted for radioactivity using a Gamma HES (γ counter; Shin Jin Medics Inc, Seoul, Korea). Uptake in the organs and tumors was expressed as the percentage of the injected dose per gram tissue (% ID/g). For blocking study, 25 μg cold ATPS mAb, 50 times larger than the dosage of radiolabeled ATPS mAb, was coinjected with 1.85 MBq ^{125}I-ATPS mAb through the tail vein and then organs were removed at 24 hours after injection.

Radioimmunotherapy With ^{131}I-ATPS mAb in Tumor Xenograft Model and 2-deoxy-2-[^{18}F]fluoro-D-glucose Positron Emission Tomography Imaging

The therapeutic efficacy of ^{131}I-ATPS mAb was evaluated in mice using MKN-45 tumor xenografts. Mice received an intravenous injection of 18.5 MBq ^{131}I-ATPS mAb (n = 7), 5 μg of isotype immunoglobulin G (IgG) (n = 6; Sigma-Aldrich, St Louis, Missouri), and vehicle (n = 6, normal saline), respectively, once a week for 4 weeks.[19] The number of animals in each group was determined by a crude method based on law of diminishing return.[20] Tumor size was measured weekly in 2 dimensions (length and width) using a caliper. Tumor volume was calculated by the formula, V = (length × width^2)/2,[21] and compared between the 2 groups. To evaluate the antitumor effect, tumor growth inhibition (TGI) was determined each week using the formula: $\%TGI = \{1 - [(T_t/T_0)/(C_t/C_0)]/1 - [C_0/C_t]\} \times 100$, where T_t and C_t are the tumor volumes of the treated and control groups at time t, respectively, whereas T_0 and C_0 are those at baseline. A median %TGI of at least 50% was considered as the cutoff for a significant antitumor effect. For imaging purpose, positron emission tomography (PET) images were acquired 1 hour after an intravenous injection of 18.5 MBq 2-deoxy-2-[^{18}F]fluoro-D-glucose (^{18}F-FDG) using a small animal PET scanner (eXplore Vista; GE healthcare, Milwaukee, Wisconsin) before and after ^{131}I-ATPS mAb therapy. Mice were scanned for 30 minutes under inhalation anesthesia using isoflurane. The tumor uptake (% ID/g) in representative PET images was calculated using AMIDE (freeware; http://amide.sourceforge.net, version 1.0.4).

Statistical Analysis

All data are presented as means ± standard errors. The statistical comparison of cellular uptake and tumor size was evaluated by Student t test and Kruskal-Wallis test using statistical software (R, version 3.1.2), and the difference was considered significant at $P < .05$.

Results

Radioiodination of ATPS mAb

The radiochemical yield of ^{125}I-ATPS mAb increased gradually with the dosage of ATPS mAb: 47.5% ± 4.0%, 69.0% ± 0.9%, 74.4% ± 0.7%, 75.9% ± 1.9%, and 91.5% ± 1.3% at 5, 10, 20, 40, and 80 μg, respectively (Figure 1A). This pattern was the same when using ^{131}I-ATPS mAb: 4.3% ± 0.9%, 17.3% ± 1.5%, 36.7% ± 3.0%, 43.3% ± 3.2%, and 52.0% ± 2.0% at 5, 10, 20, 40, and 80 μg, respectively (Figure 1B). Throughout the current study, the labeling efficiency of ^{125}I-ATPS mAb was better than that of ^{131}I-ATPS mAb. The entire labeling procedure was completed within 45 minutes.

In Vitro Cellular Uptake and Retention Rate

The cellular uptake of ^{125}I-ATPS mAb was measured in various cancer cell lines (Figure 2A). MKN-45 cells showed the highest cellular uptake at 2 hours (0.00122 ± 0.00009%/μg) and 4 hours (0.00324 ± 0.00013%/μg). The MKN-45 cellular uptake at 4 hours was significantly higher than that in the other cell lines (1.8- to 6.2-fold, all $P < .05$). Based on these results, MKN-45 cells were selected for subsequent experiments.

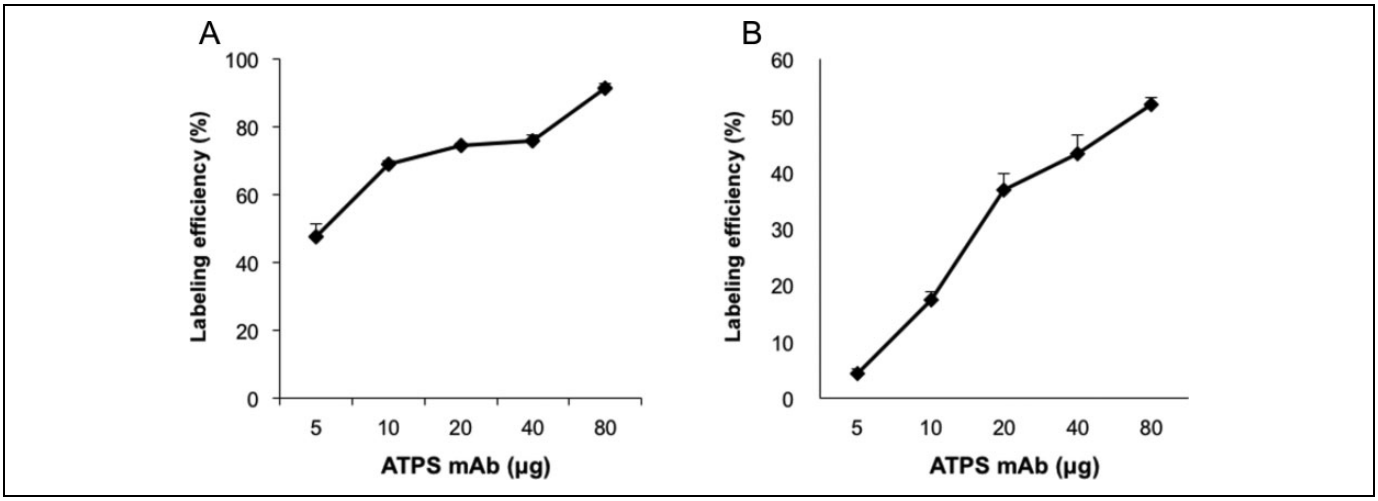

Figure 1. Radiochemical yield of ^{125}I-ATPS mAb (A) and ^{131}I-ATPS mAb (B) at various doses of ATPS mAb. Error bar = standard error. ATPS mAb indicates adenosine triphosphate synthase monoclonal antibody.

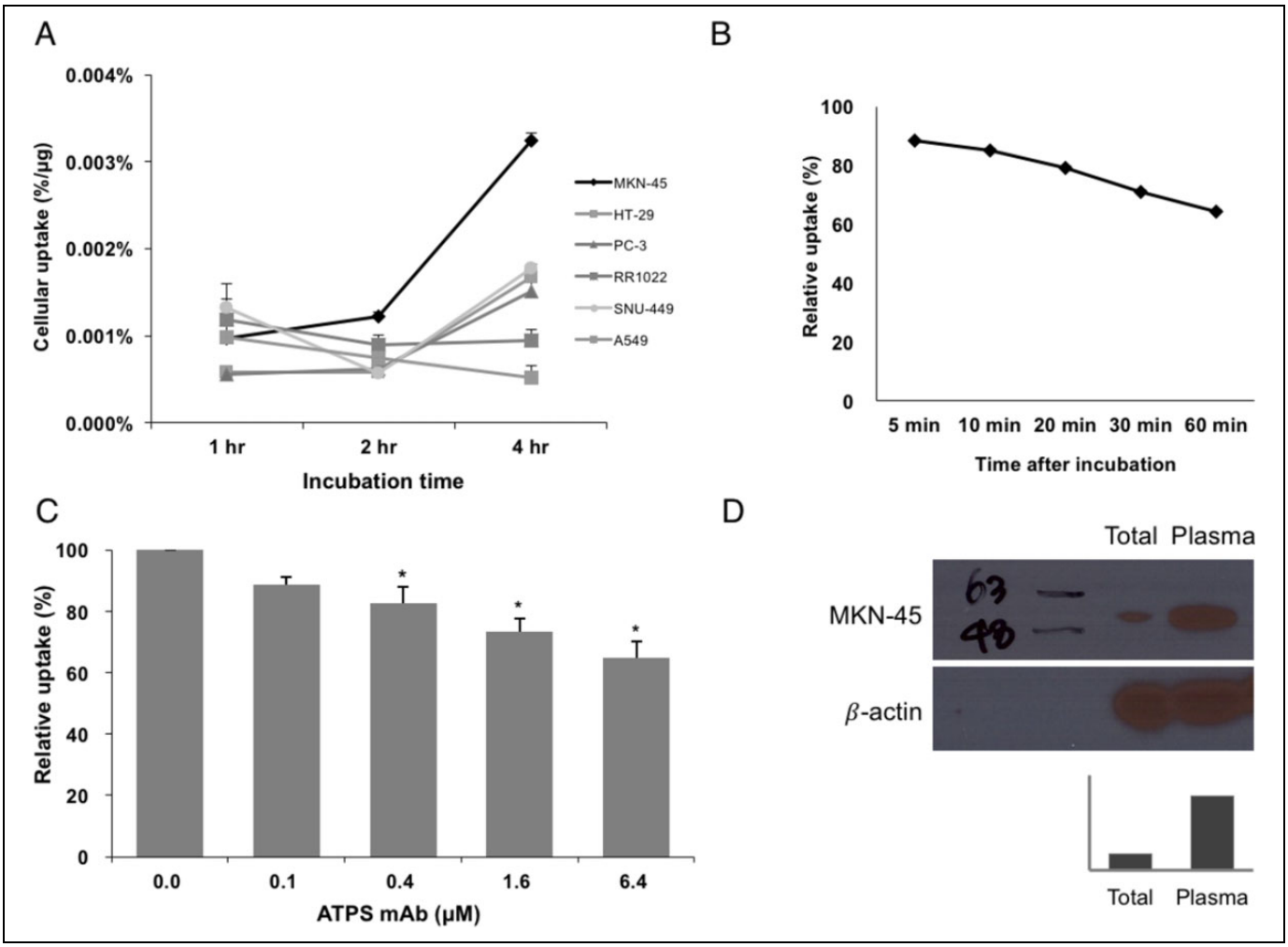

Figure 2. Cellular uptake (A) of ^{125}I-ATPS mAb in various cancer cells at 1, 2, and 4 hours of incubation and the retention rate (B) of ^{125}I-ATPS mAb in MKN-45 cells. The inhibition of cellular uptake (C) of ^{125}I-ATPS mAb in MKN-45 cells by anti-ATPS mAb. Western blot analysis (D) for adenosine triphosphate synthase was performed using anti-ATPS mAb. Protein bands were visualized for both total membranes and plasma membranes at 57 kDa (estimated by prestained protein marker). The intensity of band was 4.5 times higher for plasma membrane proteins than for total membrane proteins. *$P < .05$ compared to untreated control. Error bar = standard error. ATPS mAb indicates adenosine triphosphate synthase monoclonal antibody.

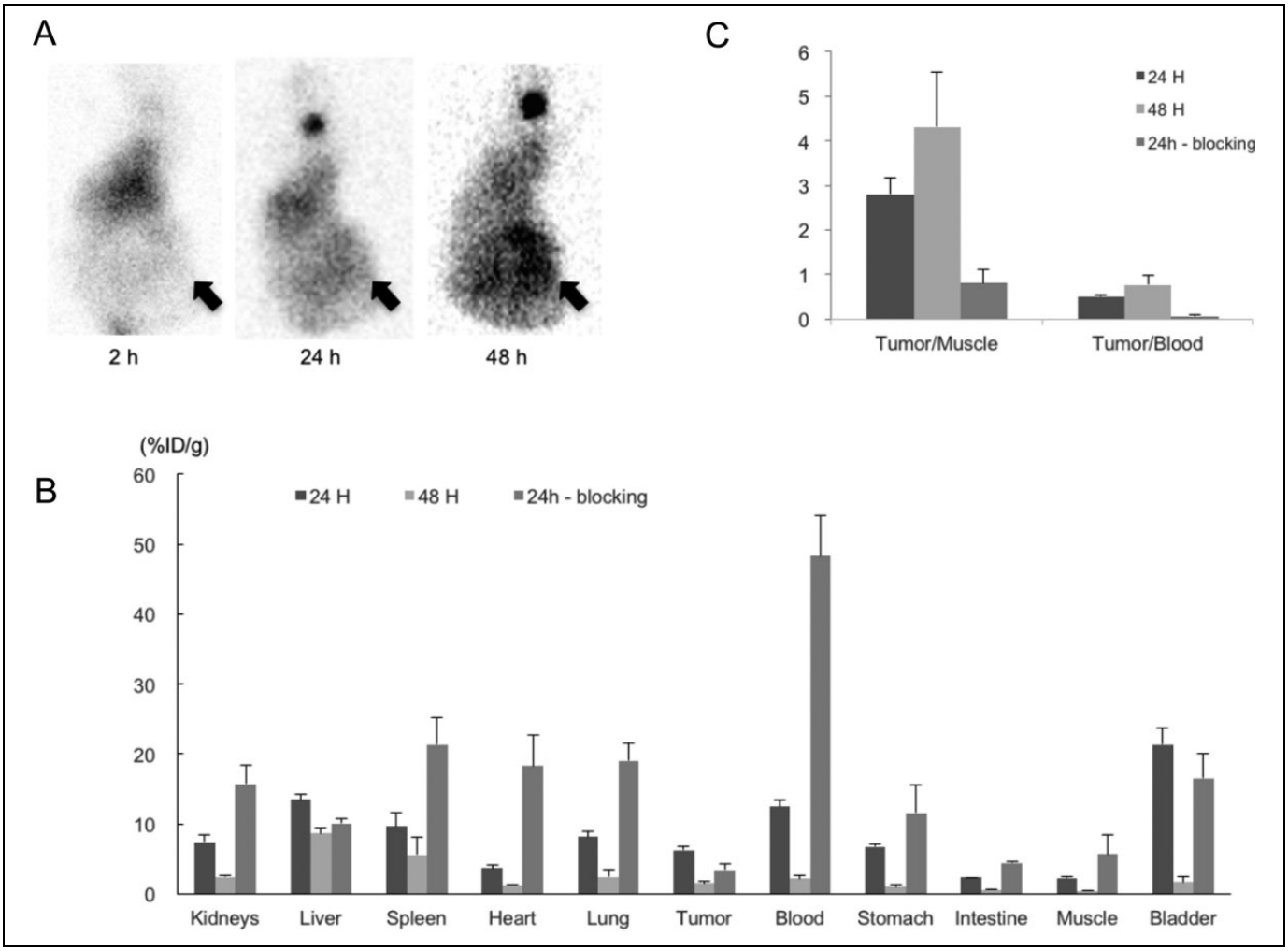

Figure 3. γ Camera images at 2, 24, and 48 hours (A) and biodistribution (B and C) at 24, 48 and 24 hours with blocking antibody. Data were acquired after intravenous injection of 3.7 MBq ^{125}I-ATPS mAb in MKN-45 tumor-bearing mice. Mice were scanned for 20 minutes in a prone position under inhalation anesthesia using isoflurane. Error bar = standard error. Arrows indicate tumors. ATPS mAb indicates adenosine triphosphate synthase monoclonal antibody.

The retention rates of ^{125}I-ATPS mAb in MKN-45 cells were 88.4% ± 0.4%, 85.1% ± 0.5%, 79.3% ± 0.8%, 70.9% ± 1.0%, and 64.1% ± 1.0% at 5, 10, 20, 30, and 60 minutes, respectively (Figure 2B). The majority of ^{125}I-ATPS mAb was retained in tumor cells at 5 minutes, and the amount retained decreased slowly over time.

Specific Inhibition of ^{125}I-ATPS mAb by Anti-ATPS mAb in MKN-45 Cells

The inhibition study showed that unlabeled ATPS mAb hindered the binding of ^{125}I-ATPS mAb to MKN-45 cells in a dose-dependent manner. Compared with the untreated control, the relative cellular binding levels of ^{125}I-ATPS mAb in treated cells were 88.7% ± 2.7%, 82.6% ± 5.3%, 73.5% ± 4.3%, and 64.9% ± 5.2% at 0.1, 0.4, 1.6, and 6.4 μM, respectively (Figure 2C). The levels of cellular binding were significantly lower in treated cells than in control cells with 0.4, 1.6, and 6.4 μM ATPS mAb (P = .033, .013, and .004, respectively). These results indicate that ^{125}I-ATPS mAb is specifically bound to MKN-45 cells in vitro.

Expression of ATP Synthase in MKN-45 Cells

Western blot analysis using anti-ATPS mAb revealed that the expression of ATP synthase was 4.5 times higher for plasma membranes than for total membranes (Figure 2D). The plasma membrane fraction was 20.0% of total membrane fraction by protein analysis. Therefore, the majority of ATP synthase was expressed on the surface of MKN-45 cells (plasma membranes to mitochondria ratio = 9:1).

γ Camera Imaging and Biodistribution of ^{125}I-ATPS mAb in MKN-45 Tumor-Bearing Mice

On γ camera images, tumor uptake was discernible from 24-hour images, and the tumor to background contrast became more pronounced at 48 hours (Figure 3A). Thyroid uptake

Table 1. Biodistribution Data for ^{125}I-ATPS mAb in Human Gastric Cancer–Bearing Nude Mice Before and After Blocking With Cold ATPS mAb.[a]

Organs	24 Hours (n = 3)	48 Hours (n = 3)	24 Hours—Blocking (n = 3)
Thyroid	2875.55 ± 51.81	1916.52 ± 173.39	
Kidneys	7.40 ± 1.00	2.42 ± 0.24	15.73 ± 2.66
Liver	13.47 ± 0.74	8.61 ± 0.77	10.08 ± 0.62
Spleen	9.67 ± 1.91	5.61 ± 2.56	21.35 ± 3.82
Heart	3.65 ± 0.46	1.26 ± 0.13	18.24 ± 4.47
Lung	8.16 ± 0.81	2.46 ± 1.07	19.00 ± 2.50
Tumor	6.26 ± 0.47	1.50 ± 0.23	3.43 ± 0.85
Blood	12.43 ± 0.98	2.18 ± 0.47	48.31 ± 5.80
Stomach	6.71 ± 0.35	1.02 ± 0.28	11.52 ± 4.04
Intestine	2.34 ± 0.02	0.61 ± 0.02	4.44 ± 0.13
Muscle	2.27 ± 0.12	0.42 ± 0.13	5.67 ± 2.80
Bladder	21.36 ± 2.34	1.69 ± 0.85	16.52 ± 3.54
Tumor/muscle[b]	2.79 ± 0.37	4.31 ± 1.22	0.81 ± 0.30
Tumor/blood[b]	0.51 ± 0.04	0.77 ± 0.21	0.07 ± 0.02

Abbreviation: ATPS mAb, adenosine triphosphate synthase monoclonal antibody.
[a]Values are given as mean ± standard error of % ID/g.
[b]Ratio.

increased gradually from 24 to 48 hours postinjection by the deiodination of ^{125}I-ATPS mAb in vivo.

The biodistribution of ^{125}I-ATPS mAb in MKN-45 tumor-bearing mice at 24 and 48 hours is displayed in Figure 3B and Table 1. The biodistribution data at 2 hours were omitted because no tumor or thyroid uptake was visualized on γ camera images. The highest tumor uptake was achieved 24 hours postinjection (6.26% ± 0.47% ID/g) and had decreased by 48 hours (1.50 ± 0.23% ID/g). On the other hand, tumor to muscle and tumor to blood ratios increased over time (Figure 3C), although the difference was not statistically significant. Tumor to muscle ratios were 2.79 ± 0.37 and 4.31 ± 1.22 at 24 and 48 hours, respectively, and tumor to blood ratios were 0.51 ± 0.04 and 0.77 ± 0.21 at 24 and 48 hours, respectively.

The radioactivity of the bladder was high at 24 hours (21.36 ± 2.34% ID/g) but declined markedly at 48 hours (1.69 ± 0.85% ID/g). The radioactivity of the other organs also decreased gradually with time.

After blocking with unlabeled ATPS mAb, tumor uptake at 24 hours significantly decreased to 3.43 ± 0.85% ID/g (Figure 3B and Table 1, $P = .0437$, compared to tumor uptake at 24 hours without blocking). Similarly, tumor/muscle ratio and tumor/blood ratio also decreased significantly to 0.81 ± 0.30 ($P = .0141$) and 0.07 ± 0.02 ($P = .0006$), respectively.

Radioimmunotherapy With ^{131}I-ATPS mAb in MKN-45 Tumor-Bearing Mice

All animals injected with ^{131}I-ATPS mAb, isotype IgG, or vehicle survived until the end of the experiment. There was no significant difference in the baseline tumor volume among the 3 groups (190.2 ± 46.8 mm^3, 196.4 ± 30.9 mm^3, and 202.7 ± 55.9 mm^3 for ^{131}I-ATPS mAb-treated, IgG-treated, and control groups, respectively, $P > .05$; Figure 4A). After 4 weeks of treatment, the tumors in the treated group (679.4 ± 232.3 mm^3) were significantly smaller than those in the control group (1687.6 ± 420.4 mm^3, $P = .0431$) and in the IgG-treated group (2870.2 ± 484.1 mm^3, $P = .0010$). The %TGI after ^{131}I-ATPS mAb treatment was over 50% for the entire study period (range: 53.7%-75.9%), and the median %TGI was 61.2% (Table 2). Representative ^{18}F-FDG PET images of each group are displayed in Figure 4B.

Discussion

In this study, ATPS mAb was labeled with radioiodine to develop a theragnostic agent against tumor angiogenesis. Among the various cancer cells evaluated, MKN-45 cells showed the highest and most specific uptake of ^{125}I-ATPS mAb. In a biodistribution study, xenograft uptake of ^{125}I-ATPS mAb peaked at 24 hours after intravenous injection; however, the contrast between tumor and background was optimal for analysis 48 hours after injection. Furthermore, ^{131}I-ATPS mAb treatment significantly suppressed the growth of MKN-45 xenografts in mice, which demonstrated the potential of ATPS mAb for radioimmunotherapy. To our knowledge, this is the first study that has evaluated the feasibility of using a radiolabeled monoclonal antibody targeting ATP synthase for imaging and tumor angiogenesis prevention.

Angiostatin is a well-known and potent angiostatic factor that inhibits the growth of preexisting micrometastases. However, angiostatin treatment requires daily injection without interruption and is difficult to produce; thus, the future of angiostatin therapy for clinical use may be limited.[22] Instead of angiostatin, recent research has focused on ectopic ATP synthase as an antiangiogenic target after it was identified as the receptor for angiostatin.[7,8]

Radioiodinated angiostatin was the first radiotracer produced that was based on the binding of angiostatin to ectopic F_1F_O ATP synthase.[3] The specific binding of ^{125}I-angiostatin to

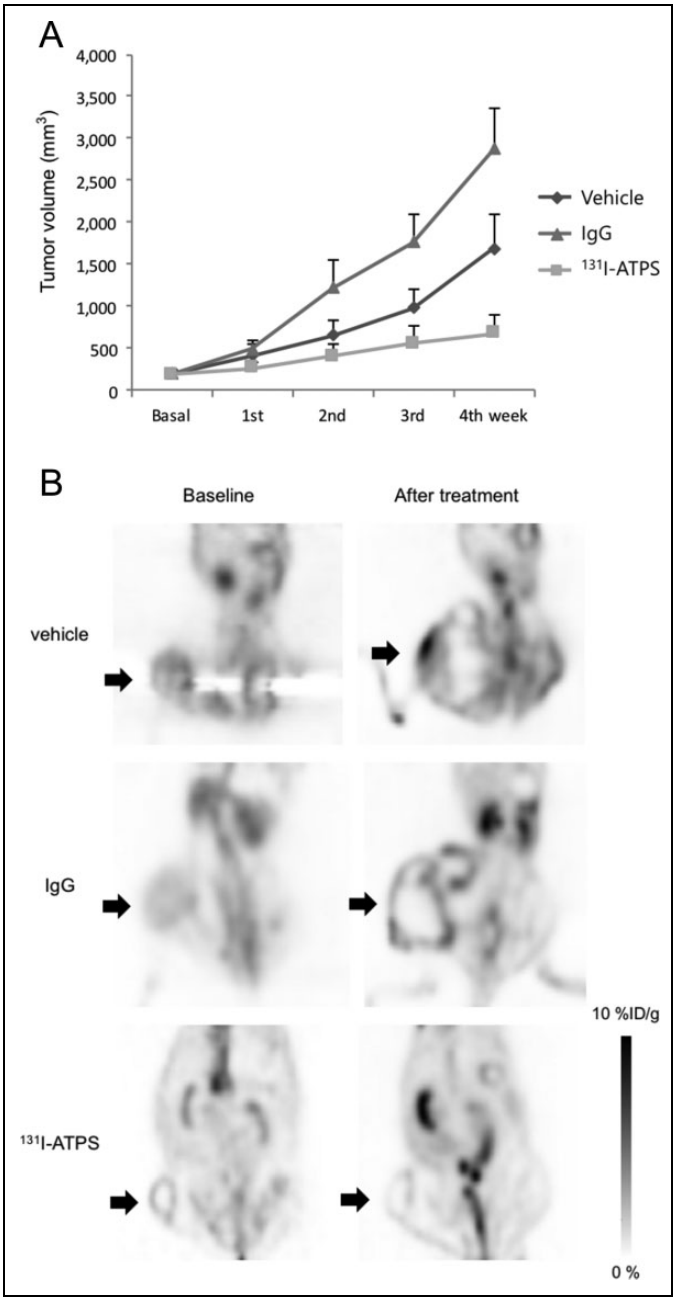

Figure 4. Changes in tumor volumes after treatment with ^{131}I-ATPS mAb, isotype IgG, or vehicle in MKN-45 tumor bearing mice (A). Error bar = standard error. Representative ^{18}F-FDG PET images obtained from each group before and after treatment (B). Positron emission tomography images were acquired 1 hour after an intravenous injection of 18.5 MBq ^{18}F-FDG. Mice were scanned for 30 minutes under inhalation anesthesia using isoflurane. Arrows indicate tumors. ATPS mAb indicates adenosine triphosphate synthase monoclonal antibody; PET, positron emission tomography.

cell surface F_1F_O ATP synthase was shown in human umbilical vein endothelial cells and human colon cancer cells.[14] Radioiodine can be attached to angiostatin either by lactoperoxidase catalysis or through covalent coupling using Bolton-Hunter reagent.[12,13] Direct labeling of angiostatin showed modest

Table 2. Tumor Growth Inhibition by ^{131}I-ATPS mAb.[a]

Time	Tumor Volume (mm^3)		%TGI
	Control	Treated Mice	
Basal	202.7 ± 55.9	190.2 ± 46.8	
1st week	419.5 ± 135.4	266.2 ± 67.8	53.7%
2nd week	660.8 ± 181.7	410.6 ± 136.6	59.2%
3rd week	980.1 ± 236.0	561.9 ± 208.7	63.2%
4th week	1687.6 ± 420.4	679.4 ± 232.3	75.9%

Abbreviations: ATPS mAb, adenosine triphosphate synthase monoclonal antibody; TGI, tumor growth inhibition.
[a]Values are given as mean ± standard error.

labeling efficiencies ranging from 40% to 70%.[12] However, the in vivo stability of radioiodinated angiostatin was so poor that thyroid uptake by deiodination appeared on γ camera images as early as 1 hour after intravenous injection. The in vivo stability of radioiodinated angiostatin was markedly improved by the Bolton-Hunter method (thyroid uptake = 15.47 ± 7.74% ID/g) compared with the direct labeling method (430.87 ± 32.17% ID/g).[13] However, the average labeling efficiency was only 20%. In comparison, the radioiodinated ATPS mAb in this study showed similar level of labeling efficiencies (76%-95% for ^{125}I and 43%-52% for ^{131}I at 40-80 μg antibody) and better in vivo stability compared to the direct labeling method. Thyroid uptake of ^{125}I-ATPS mAb was not obvious at 2 hours but became prominent after 24 hours on γ camera images. In terms of the labeling efficiency and stability, radioiodinated ATPS mAb could be an effective substitute for radioiodinated angiostatin. We also have performed the indirect radioiodination of anti-ATPS mAb using Bolton-Hunter reagent; however, we failed to conjugate it to the antibody. Free radioiodine uptake by nontarget organs can be blocked by iodide solution, which is currently used in the clinic. Therefore, the direct radioiodination is a clinically applicable labeling method for anti-ATPS mAb.

In this study, early renal excretion of ^{125}I-ATPS mAb was demonstrated during the biodistribution analysis. Bladder radioactivity was 21.36 ± 2.34% ID/g at 24 hours but dropped to 1.69 ± 0.85% ID/g at 48 hours, which may be due to the renal excretion of free iodide from the deiodination of ^{125}I-ATPS mAb. Liver uptake was also high at 24 hours (13.47 ± 0.74% ID/g) and it decreased to 8.61 ± 0.77% ID/g at 48 hours. The β-chain of ATP synthase was recently found to be expressed on the surface of hepatocytes and serves as a high-density lipoprotein receptor for apolipoprotein A-I.[23] Therefore, liver uptake of ^{125}I-ATPS mAb could be partly attributed to binding to ATP synthase on the surface of hepatocytes. However, in the presence of deiodination, liver can accumulate and metabolize radiolabeled thyroid hormones that are produced by functioning thyroids.[24] One report also suggested that the uptake of circulating antigen–antibody complexes is the primary mechanism for hepatocytes to uptake radiolabeled antibodies.[25] Therefore, the liver uptake of radioiodinated ATPS mAb imaging may not be attributed to a single mechanism.

In this study, ^{125}I was used for both a biodistribution study and γ camera, and the relatively long half-life of ^{125}I (59.4 days) has enabled the investigation of radiotracer distribution for more than 24 hours in preclinical studies. Long life in the circulation is a well-known problem for whole antibodies;[26] thus, ^{123}I ($t_{1/2}$ = 13.2 hours) is not appropriate for the evaluation of long-term biodistribution. However, ^{125}I emits low-energy photons that are inappropriate for γ camera imaging. An optimal radioisotope tracer combination for ATPS mAb imaging needs to be investigated further. Considering the late tumor binding of ATPS mAb, ^{111}In ($t_{1/2}$ = 2.80 days), ^{67}Ga ($t_{1/2}$ = 3.26 days), and ^{177}Lu ($t_{1/2}$ = 6.75 days) are radioisotope candidates that may be used in γ camera imaging.[27-30] All of these radioisotopes are metal cations that require a functional group to conjugate to antibodies. Among the radioiodines, ^{124}I ($t_{1/2}$ = 4.20 days), a positron emitter, is suitable for long-term imaging.[31] However, according to our preliminary results, the labeling of ^{124}I-ATPS mAb is a challenging work because of its low radiochemical yield and specific activity.

Using long-lived radioisotopes and the forced clearance of unbound radiopharmaceuticals are important to enhance the quality of monoclonal antibody images. In this study, while ^{125}I-ATPS mAb attained a peak tumor uptake after 24 hours, the maximal tumor to background ratio was achieved after 48 hours. A previous report showed that the clearance rate of IgG monoclonal antibodies is influenced by serum concentration.[32] Intravenous injection of immunoglobulin enhanced the clearance of monoclonal antibodies ~2-fold through the saturation of the FcRn salvage receptor.[33] Therefore, pretreatment with immunoglobulin may be a possible strategy to achieve an early tumor to background peak for radioiodinated ATPS mAb.

Radioimmunotherapy is a novel anticancer treatment based on antibody-mediated specific delivery of radiation to improve therapeutic efficacy and minimize toxicity to normal tissues. Radiolabeled anti-CD20 monoclonal antibodies such as Bexxar and Zevalin have been approved for clinical use in non-Hodgkin's lymphoma after ascertaining the therapeutic efficacy as a single agent.[34-37] However, radioimmunotherapy for solid tumors has been only a partial success in patients with minimal residual disease and micrometastasis and needs to be optimized further.[38,39] We evaluated the antitumor effect of ^{131}I-ATPS mAb in stomach cancer–xenografted mice. The results showed that ^{131}I-ATPS mAb significantly suppressed tumor growth in comparison with isotype IgG or vehicle after 4 weeks. The amount of mAb used for radioimmunotherapy in this study is only 5 μg, which was too small to exert therapeutic effects on the tumor growth compared to the previous reports.[40,41] Therefore, the inhibitory effect on the tumor growth during the radioimmunotherapy probably came from β-radiation, not from mAb itself. The %TGI was greater than 50% during the first week of treatment and then increased with repeated treatment. However, ^{131}I-ATPS mAb did not completely suppress tumor growth in the treated group (190.2 ± 46.8 mm^3 at baseline to 679.4 ± 232.3 mm^3 by week 4). Since only a single protocol (18.5 MBq ^{131}I-ATPS mAb once a week for 4 weeks) in a single disease model was evaluated in this study, a protocol adjustment, as well as evaluation in different disease models, is required. In addition, strategies combining radiolabeled antibody treatment with chemotherapeutic or cytostatic agents should also be considered.

Targeting angiogenesis for the treatment of stomach cancer has been attempted clinically using several different types of antiangiogenic agents: ligands for vascular endothelial growth factor (VEGF), VEGF receptor 2 antagonists, and receptor tyrosine kinase inhibitors.[42] The survival benefit of the VEGF ligand has only been shown in Western countries and not in the general population. Receptor tyrosine kinases also showed no therapeutic effects as single agents and have so far not been entered into stage III clinical trials. Among these treatments, only the VEGF receptor 2 antagonist ramucirumab had an effect both as a single agent and in combination with paclitaxel, regardless of race. Therefore, the development of a new antiangiogenesis therapy with a different target is essential for stomach cancer. Results from this study suggest that radioiodinated ATPS mAb is a good candidate for antiangiogenic treatment in stomach cancer.

Using whole mouse IgG for ATP synthase is a limitation of this study. As mentioned above, the long-term blood circulation, up to 3 weeks in humans, is a problematic characteristic of whole antibodies and results in high background in imaging and significant toxicity to normal tissues.[43] In addition, the human antimouse antibody response is also a problem encountered when using mouse monoclonal antibodies. Low in vivo stability of radioiodinated ATPS and the subsequent high thyroid uptake also need to be improved, although it was better than that of radioiodinated angiostatin. Researchers have developed various engineered antibodies by downsizing, multimerization, or humanization to improve circulation, binding affinity, tissue penetration, and in vivo stability.[44-46] This is a preliminary study to investigate the feasibility of using ATPS mAb for both radionuclide imaging and radioimmunotherapy; therefore, further technical enhancement is necessary before a radioiodinated ATPS mAb can be tested in clinics.

Conclusion

Adenosine triphosphate synthase monoclonal antibody was labeled with radioiodine with a sufficient radiochemical yield and showed a specific uptake and therapeutic effect in stomach cancer. Although the feasibility of radioiodinated ATPS mAb as a theragnostic agent targeting angiogenesis was proven in this study, further studies are needed to improve the biodistribution and therapeutic efficacy.

Declaration of Conflicting Interests

The author(s) declared no potential conflicts of interest with respect to the research, authorship, and/or publication of this article.

Funding

The author(s) disclosed receipt of the following financial support for the research, authorship, and/or publication of this article: This study

was supported by the grants from National Research Foundation of Korea (NRF) funded by the Korean government (MEST; NRF-2012R1A1A3015149 and NRF-2013R1A1A1061661).

References

1. Folkman J. Tumor angiogenesis: therapeutic implications. *N Engl J Med*. 1971;285(21):1182–1186.
2. Folkman J. Role of angiogenesis in tumor growth and metastasis. *Semin Oncol*. 2002;29(6 suppl 16):15–18.
3. Moser TL, Stack MS, Asplin I, et al. Angiostatin binds ATP synthase on the surface of human endothelial cells. *Proc Natl Acad Sci U S A*. 1999;96(6):2811–2816.
4. Ma Z, Cao M, Liu Y, et al. Mitochondrial F1Fo-ATP synthase translocates to cell surface in hepatocytes and has high activity in tumor-like acidic and hypoxic environment. *Acta Biochim Biophys Sin (Shanghai)*. 2010;42(8):530–537.
5. Kenan DJ, Wahl ML. Ectopic localization of mitochondrial ATP synthase: a target for anti-angiogenesis intervention? *J Bioenerg Biomembr*. 2005;37(6):461–465.
6. Moser TL, Kenan DJ, Ashley TA, et al. Endothelial cell surface F1-F0 ATP synthase is active in ATP synthesis and is inhibited by angiostatin. *Proc Natl Acad Sci U S A*. 2001;98(12): 6656–6661.
7. Chi SL, Wahl ML, Mowery YM, et al. Angiostatin-like activity of a monoclonal antibody to the catalytic subunit of F1F0 ATP synthase. *Cancer Res*. 2007;67(10):4716–24.
8. Zhang X, Gao F, Yu LL, et al. Dual functions of a monoclonal antibody against cell surface F1F0 ATP synthase on both HUVEC and tumor cells. *Acta Pharmacol Sin*. 2008;29(8): 942–950.
9. Sharkey RM, Goldenberg DM. Cancer radioimmunotherapy. *Immunotherapy*. 2011;3(3):349–370.
10. Goldenberg DM, DeLand F, Kim E, et al. Use of radiolabeled antibodies to carcinoembryonic antigen for the detection and localization of diverse cancers by external photoscanning. *N Engl J Med*. 1978;298(25):1384–1386.
11. Goldenberg DM, Gaffar SA, Bennett SJ, Beach JL. Experimental radioimmunotherapy of a xenografted human colonic tumor (GW-39) producing carcinoembryonic antigen. *Cancer Res*. 1981;41(11 pt 1):4354–4360.
12. Lee KH, Song SH, Paik JY, et al. Specific endothelial binding and tumor uptake of radiolabeled angiostatin. *Eur J Nucl Med Mol Imaging*. 2003;30(7):1032–1037.
13. Song SH, Jung KH, Paik JY, et al. Distribution and pharmacokinetic analysis of angiostatin radioiodine labeled with high stability. *Nucl Med Biol*. 2005;32(8):845–850.
14. Jung KH, Song SH, Paik JY, et al. Direct targeting of tumor cell F(1)F(0) ATP-synthase by radioiodine angiostatin in vitro and in vivo. *Cancer Biother Radiopharm*. 2007;22(5):704–712.
15. Hnatowich DJ, Childs RL, Lanteigne D, Najafi A. The preparation of DTPA-coupled antibodies radiolabeled with metallic radionuclides: an improved method. *J Immunol Methods*. 1983; 65(1-2):147–157.
16. Smith-Jones PM, Vallabhajosula S, Navarro V, Bastidas D, Goldsmith SJ, Bander NH. Radiolabeled monoclonal antibodies specific to the extracellular domain of prostate-specific membrane antigen: preclinical studies in nude mice bearing LNCaP human prostate tumor. *J Nucl Med*. 2003;44(4):610–617.
17. Stollman TH, Scheer MG, Leenders WP, et al. Specific imaging of VEGF-A expression with radiolabeled anti-VEGF monoclonal antibody. *Int J Cancer*. 2008;122(10):2310–2314.
18. Bradford MM. A rapid and sensitive method for the quantitation of microgram quantities of protein utilizing the principle of protein-dye binding. *Anal Biochem*. 1976;72:248–254.
19. Molthoff CF, Pinedo HM, Schluper HM, Boven E. Influence of dose and schedule on the therapeutic efficacy of 131I-labelled monoclonal antibody 139H2 in a human ovarian cancer xenograft model. *Int J Cancer*. 1992;50(3):474–480.
20. Charan J, Kantharia ND. How to calculate sample size in animal studies? *J Pharmacol Pharmacother*. 2013;4(4):303–306.
21. Bhagwat SV, Gokhale PC, Crew AP, et al. Preclinical characterization of OSI-027, a potent and selective inhibitor of mTORC1 and mTORC2: distinct from rapamycin. *Mol Cancer Ther*. 2011; 10(8):1394–1406.
22. Wahl ML, Kenan DJ, Gonzalez-Gronow M, Pizzo SV. Angiostatin's molecular mechanism: aspects of specificity and regulation elucidated. *J Cell Biochem*. 2005;96(2):242–261.
23. Martinez LO, Jacquet S, Esteve JP, et al. Ectopic beta-chain of ATP synthase is an apolipoprotein A-I receptor in hepatic HDL endocytosis. *Nature*. 2003;421(6918):75–79.
24. Chung JK, Lee YJ, Jeong JM, et al. Clinical significance of hepatic visualization on iodine-131 whole-body scan in patients with thyroid carcinoma. *J Nucl Med*. 1997;38(8):1191–1195.
25. Beatty BG, O'Conner-Tressel M, Do T, Paxton RJ, Beatty JD. Mechanism of decreasing liver uptake of 111In-labeled anti-carcinoembryonic antigen monoclonal antibody by specific antibody pretreatment in tumor bearing mice. *Cancer Res*. 1990; 50(3 suppl):846s–851s.
26. Hoppin J, Orcutt KD, Hesterman JY, et al. Assessing antibody pharmacokinetics in mice with in vivo imaging. *J Pharmacol Exp Ther*. 2011;337(2):350–358.
27. Anderson WT, Strand M. Stability, targeting, and biodistribution of scandium-46- and gallium-67-labeled monoclonal antibody in erythroleukemic mice. *Cancer Res*. 1985;45(5): 2154–2158.
28. Li L, Bading J, Yazaki PJ, et al. A versatile bifunctional chelate for radiolabeling humanized anti-CEA antibody with In-111 and Cu-64 at either thiol or amino groups: PET imaging of CEA-positive tumors with whole antibodies. *Bioconjug Chem*. 2008; 19(1):89–96.
29. Grunberg J, Novak-Hofer I, Honer M, et al. In vivo evaluation of 177Lu- and 67/64Cu-labeled recombinant fragments of antibody chCE7 for radioimmunotherapy and PET imaging of L1-CAM-positive tumors. *Clin Cancer Res*. 2005;11(14): 5112–5120.
30. Dash A, Pillai MR, Knapp FF Jr. Production of (177)Lu for targeted radionuclide therapy: available options. *Nucl Med Mol Imaging*. 2015;49(2):85–107.
31. Lee FT, O'Keefe GJ, Gan HK, et al. Immuno-PET quantitation of de2-7 epidermal growth factor receptor expression in glioma using 124I-IMP-R4-labeled antibody ch806. *J Nucl Med*. 2010; 51(6):967–972.

32. Tabrizi M, Bornstein GG, Suria H. Biodistribution mechanisms of therapeutic monoclonal antibodies in health and disease. *AAPS J*. 2010;12(1):33–43.
33. Hansen RJ, Balthasar JP. Effects of intravenous immunoglobulin on platelet count and antiplatelet antibody disposition in a rat model of immune thrombocytopenia. *Blood*. 2002;100(6):2087–2093.
34. Kaminski MS, Estes J, Zasadny KR, et al. Radioimmunotherapy with iodine (131)I tositumomab for relapsed or refractory B-cell non-Hodgkin lymphoma: updated results and long-term follow-up of the University of Michigan experience. *Blood*. 2000;96(4): 259–266.
35. Kaminski MS, Zasadny KR, Francis IR, et al. Iodine-131-anti-B1 radioimmunotherapy for B-cell lymphoma. *J Clin Oncol*. 1996; 14(7):1974–1981.
36. Wiseman GA, White CA, Witzig TE, et al. Radioimmunotherapy of relapsed non-Hodgkin's lymphoma with zevalin, a 90Y-labeled anti-CD20 monoclonal antibody. *Clin Cancer Res*. 1999;5(10 suppl):3281s–3286s.
37. Witzig TE, Gordon LI, Cabanillas F, et al. Randomized controlled trial of yttrium-90-labeled ibritumomab tiuxetan radioimmunotherapy versus rituximab immunotherapy for patients with relapsed or refractory low-grade, follicular, or transformed B-cell non-Hodgkin's lymphoma. *J Clin Oncol*. 2002;20(10):2453–2463.
38. Goldenberg DM. Advancing role of radiolabeled antibodies in the therapy of cancer. *Cancer Immunol Immunother*. 2003;52(5): 281–296.
39. Jain M, Venkatraman G, Batra SK. Optimization of radioimmunotherapy of solid tumors: biological impediments and their modulation. *Clin Cancer Res*. 2007;13(5):1374–1382.
40. Wang J, Han Y, Liang J, et al. Effect of a novel inhibitory mAb against beta-subunit of F1F0 ATPase on HCC. *Cancer Biol Ther*. 2008;7(11):1829–1835.
41. Salaun PY, Bodet-Milin C, Frampas E, et al. Toxicity and efficacy of combined radioimmunotherapy and bevacizumab in a mouse model of medullary thyroid carcinoma. *Cancer*. 2010;116(4 suppl):1053–1058.
42. O'Neil B, McCarthy T. Angiogenesis inhibitors in gastric cancer. *Orphan Drugs*. 2014;4:55–61.
43. Batra SK, Jain M, Wittel UA, Chauhan SC, Colcher D. Pharmacokinetics and biodistribution of genetically engineered antibodies. *Curr Opin Biotechnol*. 2002;13(6):603–608.
44. Herbst RS, Hong WK. IMC-C225, an anti-epidermal growth factor receptor monoclonal antibody for treatment of head and neck cancer. *Semin Oncol*. 2002;29:18–30.
45. Kashmiri SV, Iwahashi M, Tamura M, Padlan EA, Milenic DE, Schlom J. Development of a minimally immunogenic variant of humanized anti-carcinoma monoclonal antibody CC49. *Crit Rev Oncol Hematol*. 2001;38(1):3–16.
46. Yazaki PJ, Wu AM, Tsai SW, et al. Tumor targeting of radiometal labeled anti-CEA recombinant T84.66 diabody and t84.66 minibody: comparison to radioiodinated fragments. *Bioconjug Chem*. 2001;12(2):220–228.